

The 3D structure of the tectorial membrane determined by second-harmonic imaging microscopy

Rachel Gueta ^{a,1}, Eran Tal ^{b,1}, Yaron Silberberg ^b, Itay Rouso ^{a,*}

^a Department of Structural Biology, Weizmann Institute of Science, 76100 Rehovot, Israel

^b Department of Physics of Complex Systems, Weizmann Institute of Science, 76100 Rehovot, Israel

Received 14 November 2006; received in revised form 25 February 2007; accepted 2 March 2007

Available online 24 March 2007

Abstract

The tectorial membrane (TM) is a highly hydrated non-cellular matrix situated over the sensory cells of the cochlea. It is widely accepted that the mechanical coupling, between the TM and outer hair cells stereocilia bundles, plays an important role in the cochlea energy transduction mechanism. Recently, we provided supporting evidence for the existence of mechanical coupling by demonstrating that the mechanical properties of the TM change along its longitudinal direction. Since the biochemical composition of the TM is similar throughout its entire length, it is likely that structural differences induce the observed material properties changes. Presently, however, the structure of the TM under physiological environments remains unknown. In this work, the 3D structure of native TM samples is shown by using two-photon second-harmonic imaging microscopy. We find that the collagen fibers at the basal region are arranged in a parallel orientation while being tilted in an angle with respect to the plane of the TM surface at the apical region. Moreover, we find an intensified marginal band at the basal OHC zone which forms a shell-like structure which engulfs the stereocilium imprints surface of the TM. In supports of our previous mechanical characterization, the analysis presented here provides a structural basis for the changes in TM's mechanical properties.

© 2007 Elsevier Inc. All rights reserved.

Keywords: Collagen fibers; Hearing; Cochlea; Tectorial membrane; Second-harmonic microscopy

1. Introduction

The cochlea is the mammalian organ that transduces mechanical audio stimuli into an electrical signal, which then stimulates the brain via the auditory nerve. During auditory stimulation, the stereocilium bundles of the sensory cells—outer hair cells (OHCs)² and inner hair cells (IHCs)—are pushed against the tectorial membrane (TM), an extracellular matrix that spans the entire length of the cochlea and is situated over the sensory cells (Fig. 1). Mechanical interactions between the TM and the bundles of stereocilia cause deflection of the bundles. The

induced deflection is the impulse that converts the audio-induced mechanical motion into an electrical signal. The significance of the TM in hearing is indicated by the fact that mutations in proteins of the TM cause auditory impairments (Jacobson et al., 1990; Legan et al., 1997, 2005; McGuirt et al., 1999; Pfister et al., 2004).

The TM is a highly hydrated matrix in which water accounts for nearly 97% of its weight. The remaining 3% is made up of proteins and proteoglycans (Thalmann et al., 1993). Approximately, half of these proteins are collagenous proteins, primarily type II, with smaller amounts of collagen types V, IX, and XI. At the TM surface that faces the sensory cells, collagen type II proteins form fibrils that are assembled along the radial direction (Fig. 1A). On the opposite surface of the TM the collagen proteins fibrils are arranged in a mesh-like structure known as the covering net.

* Corresponding author. Fax: +972 8 9344136.

E-mail address: itay.rousso@weizmann.ac.il (I. Rouso).

¹ These authors contributed equally to this work.

² Abbreviations: SHIM, second-harmonic imaging microscopy; TM, tectorial membrane; OHC, outer hair cells; IHC, inner hair cells.

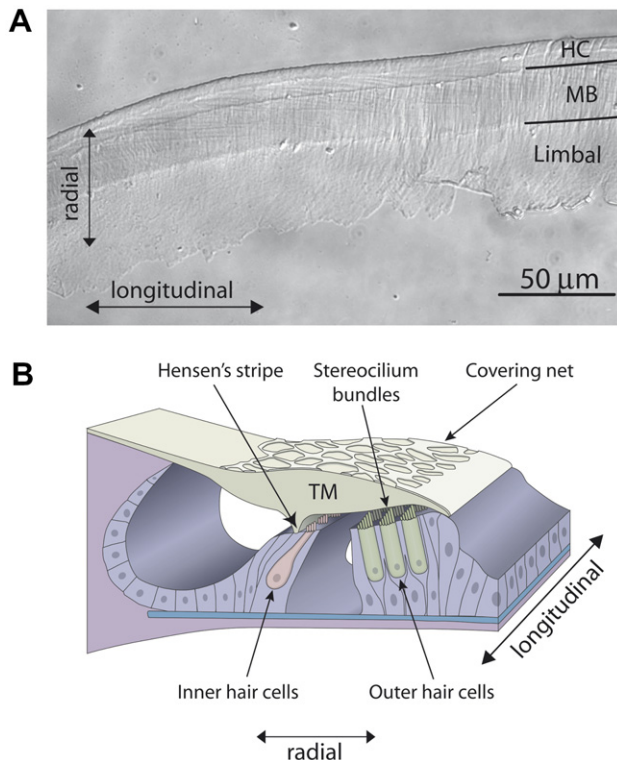


Fig. 1. (A) A phase-contrast transmitted light microscope image of a TM sample isolated from the basal region of the cochlea. The three radial zones are the outer hair cell zone ('HC'), the TM's main body ('MB'), and the spiral limbus attachment area of the TM to the cochlea ('Limbal'). (B) Schematic representation of the organ of Corti, showing the location of the TM in relation to the outer and inner hair cells in the cochlea. Longitudinal and radial directions of the TM are shown with double-headed arrows.

The ultrastructural organization of the collagen fibers in the TM has been extensively studied using various EM techniques (Arima et al., 1990; Glueckert et al., 2005; Hasko and Richardson, 1988; Slepecky et al., 1992; Thalmann et al., 1987; Tsuprun and Santi, 1997; Weaver and Schweitzer, 1994). However, sample preparation procedures for EM analysis include fixation and often require staining. Unfortunately, these treatments are likely to impair the integrity and structure of samples, particularly in the case of a highly hydrated sample such as the TM. Fixed TM samples indeed undergo significant changes, primarily sample shrinkage (Ulfendahl et al., 2001). Consequently, despite the vast body of structural information available from structural analyses, the structure—and particularly the collagen fiber arrangement—of native untreated TM under physiological environment remains unknown.

In this work we analyzed, for the first time, the 3D organization of collagen fibers along the radial and longitudinal directions of native non-treated TM samples, by using second-harmonic imaging microscopy (SHIM). SHIM is based on a nonlinear optical effect called second-harmonic generation (SHG). When light of high intensity (typically above several GW/cm^2) is focused inside a non-centrosym-

metric material, photons with a frequency equal to twice the pumping laser frequency are generated coherently. Since biological material can be assembled in a large, ordered non-centrosymmetric structure, SHIM is becoming increasingly recognized as a powerful tool for visualizing biomolecular structures in cells, tissues, and organisms (Campagnola and Loew, 2003; Millard et al., 2003). Like conventional optical microscopy, SHIM can be carried out in a physiological environment. However, SHIM has important advantages over traditional (single photon) fluorescence microscopy: (a) the wavelength of the illuminating laser is typically in the infrared range, enabling much deeper sample penetration (up to 500 μm), and (b) labeling or staining of the sample is not required. Collagen fibers are non-centrosymmetric assemblies and thus produce a good SHG signal (Freund et al., 1986), which has been used to generate SHIM images of collagen fibers either *in situ* or isolated (Cox et al., 2003; Mohler et al., 2003; Williams et al., 2005; Yasui et al., 2004; Yeh et al., 2005; Zipfel et al., 2003). (c) SHG is generated only at the focus of the pumping laser beam, where the laser power is strong enough for nonlinear effects to take place. Therefore, depth sectioning is an inherent property of SHIM—no confocal pinholes are required. For all of these reasons, SHIM is a particularly powerful technique for analysis of the native structure of the TM.

Our SHIM analysis indicates significant changes in organization of the fibers along the longitudinal direction of the TM. At the TM's apical region the collagen fibers are oriented at an angle with respect to the sample's surface. In contrast, at the basal region the fibers are thinner and are tightly arranged in parallel orientation with respect to each other and to the plane of the TM's surface. Interestingly, along the edge of the TM in the basal OHC zone we find an intensified signal, which appears to represent merging of several fibers into thick fibers. This marginal band forms a shell-like structure that engulfs the surface of the TM in this region. The results presented in this report establish a correlation between the structure and the mechanical properties of the TM.

2. Materials and methods

2.1. Sample preparation

TM samples were isolated from a six adult mice aged approximately 2 months. The mice were asphyxiated by CO_2 and their cochleas were dissected and excised using a previously reported technique (Abnet and Freeman, 2000). The isolated cochleas were immediately immersed in artificial endolymph (AE) buffer (175 mM KCl, 0.02 mM CaCl_2 , 5 mM HEPES, 2 mM NaCl, pH 7.3). A scalpel blade was used to chip away the cochlea until the organ of Corti was exposed. The TM was isolated using an eyelash manipulator under a dissection microscope with dark-field illumination. Isolated TM pieces were transferred by micropipette to a glass slide coated with

Cell-Tak (BD Biosciences, Bedford, MA) and gently tapped with an eyelash manipulator to facilitate adhesion of the tissue to the bottom of the glass chamber. The total number of TM samples analyzed in this study was nine, from which, five fragments were isolated from the apical end of the cochlea and four from the basal end.

2.2. Second-harmonic imaging microscopy

SHIM experiments were performed using an optical microscope (Axiovert 135, Carl Zeiss, Germany), modified for use as a scanning microscope. The laser source was a Tsunami[®] Ti:Sapphire femtosecond oscillator (Spectra Physics–Newport, Mountain View, CA), which delivers linearly polarized 100-fs pulses centered around 810 nm at a repetition rate of 80 MHz. The laser beam is coupled through one of the microscope ports and is focused into the sample by a 100×/1.4 numerical aperture objective lens. Pumping powers measured just before the objective were around 30. The focal point was scanned in the *xy* plane using two optical scanners, and along the *z*-axis using the microscope's motorized objective turret. The SHG signal at ~405 nm was collected by a condenser, filtered by a color glass and a narrow-band interference filter (F20-400, CVI), and measured by a photomultiplier tube (Hamamatsu R4220). The pumping laser wavelength was chosen to be 810 nm to maximize the SHG and minimize auto-fluorescence signals collected by the interference filter. The current generated by the photomultiplier is measured by use of a lock-in amplifier (model 7265, Signal Recovery–Ametek, Oak Ridge, TN). The output signal from the lock-in amplifier is fed into a computer running LabView (National Instruments, Austin, TX), which synchronizes the scanning process and the data collection. To verify that the collected signal is indeed nonlinear, we confirmed that its intensity grows quadratically with the pumping power. The scanned area of all images was 30 × 30 μm, 140 × 140 pixels. Images were acquired at 2-μm intervals throughout the entire thickness of the sample, and were processed and rendered using Imaris[®] Imaging Software (Bitplane, Zurich, Switzerland).

3. Results and discussion

Fresh TM samples were imaged in an AE buffer environment approximately 1–2 h after they were isolated from the cochlea. TM samples isolated from the apical and basilar turns were identified on the basis of their dimensions: narrow and thin samples were considered to be derived from the basal region of the cochlea, and wider and thicker samples from the apical end. In addition to its longitudinal assignment, each TM sample was subdivided into three radial zones: (a) HC, representing the location of the region with imprints of OHC stereocilium bundles, (b) MB, representing the main body of the TM, which is located approximately above the IHCs, and (c) limbal, representing the zone at which the TM is attached to the spiral limbus.

Radial zones were assigned by inspecting the sample using transmission light microscopy (Fig. 1A).

SHIM images of samples isolated from the apical region of the cochlea are shown in Fig. 2. Analysis of the fiber arrangements in the HC and MB zones shows no significant differences between these two radial zones. On both sides of the TM the arrangement of collagen fibers at the surface is parallel to the TM's surface plane (Fig. 2A, C, and F). At or near the surface, however, the fibers at the MB zone appear to be thicker than those at the HC zone (compare Fig. 2C and F). Image analysis reveals that the surface fibers at the MB have an averaged diameter of $1.1 \pm 0.3 \mu\text{m}$, while their averaged diameter at the HC zone is $0.70 \pm 0.15 \mu\text{m}$. In contrast to the arrangement of the surface fibers, in the interior of the TM the collagen fibers are tilted at an angle with respect to the surface of the TM. This is indicated by the appearance of short fragments of fibers (Fig. 2B and D). Similar short fragments are seen throughout the entire thickness of the TM (data not shown). The transition from parallel to tilted orientation is clearly shown in Fig. 2E. It is likely that imaging of this transition was achievable because of the topographic contour of the TM, so that a single optical section captured both the parallel orientation of the surface fibers and the tilted orientation of fibers in the TM interior. The transition from parallel to tilted orientation was relatively sharp and occurred within a single Z-step (2 μm). Examination of the density of collagen fibers inside the body of the TM at the HC and the MB zones reveals that fiber density at the HC zone (Fig. 2B) is substantially greater than in the MB zone (Fig. 2D).

At the basal region of the TM the fibers in the HC zone appear to be thinner (their averaged diameter is $0.4 \pm 0.1 \mu\text{m}$) than those at the apical region, and their orientation is seen to be strictly parallel, both to the plane of the TM surface and to each other (Fig. 3). In contrast to the arrangement in the apical region, this parallel orientation persists throughout the entire thickness of the TM. Interestingly, at the edge of the HC zone at the basal region of all analyzed TM samples we can see that the signal is intensified. This intensified band is probably the result of merging of fibers at the edge of the HC zone. Structural analysis of the TM over its entire thickness shows that this band exists at the edge of the TM in all of the optical Z-sections. The band begins at the TM surface that faces the OHC stereocilium (Fig. 3A), and outlines the periphery of the TM (Fig. 3B and C) until it disappears towards the opposite side (the side of the covering net) (Fig. 3D). A 3D reconstruction of the basal HC zone shows that the intensified band forms an external shell-like structure (shown in Fig. 4), which probably consist of thick and dense fibers. During sample preparation we made no attempt to control the orientation of the TM samples. Therefore, the covering net could face either away from the glass slide or towards it. Nonetheless, the orientation of the TM did not affect its observed convex shape in the basal HC zone. Figs. 3 and 4 show that even when the

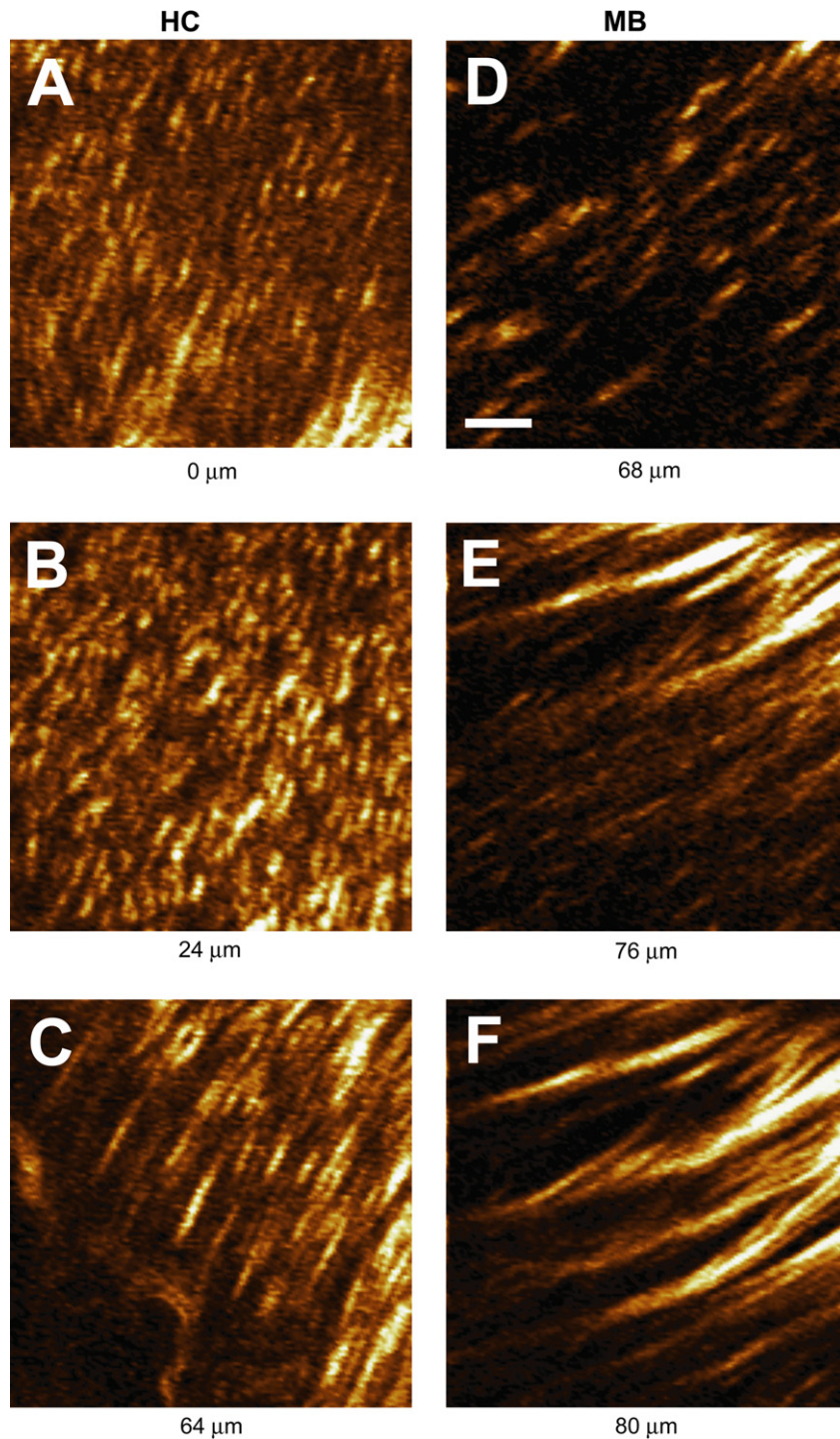


Fig. 2. Second-harmonic microscopy Z-section image series of the apical region of the TM taken at the HC zone (A–C) and the MB zone (D–F). The relative Z position of each image is shown in microns. The Z positions of the sections were shifted so that 0 μm represents the stereocilium-imprint surface of the TM. Collagen fibers at the surface of the TM are mostly arranged in parallel orientation (A, C, and F). Short fragments of fibers are primarily visible throughout the interior of the TM (B and D), suggesting that the fibers are tilted at an angle with respect to the microscope's optical plane. Transition from parallel to tilted orientation is shown in (E). The image scan area is $30 \times 30 \mu\text{m}$, 140×140 pixels. Scale bar, 5 μm . Sample thickness vary between 64–74 μm and 80–88 μm , for the HC and MB zones, respectively.

narrower side of the TM (the side facing the OHCs) was attached to the glass, the upper and wider part of the TM maintained its shape and did not collapse down towards the glass slide. On the basis of the above results, we suggest that the external shell-like structure increases

the mechanical stability and stiffness of the TM structure at the basal HC zone. It is worth mentioning that the shape of the shell-like structure fits nicely into the organ of Corti, since its slope is very similar to the tilted orientation of the corresponding OHCs (schematically illustrated in Fig. 4C).

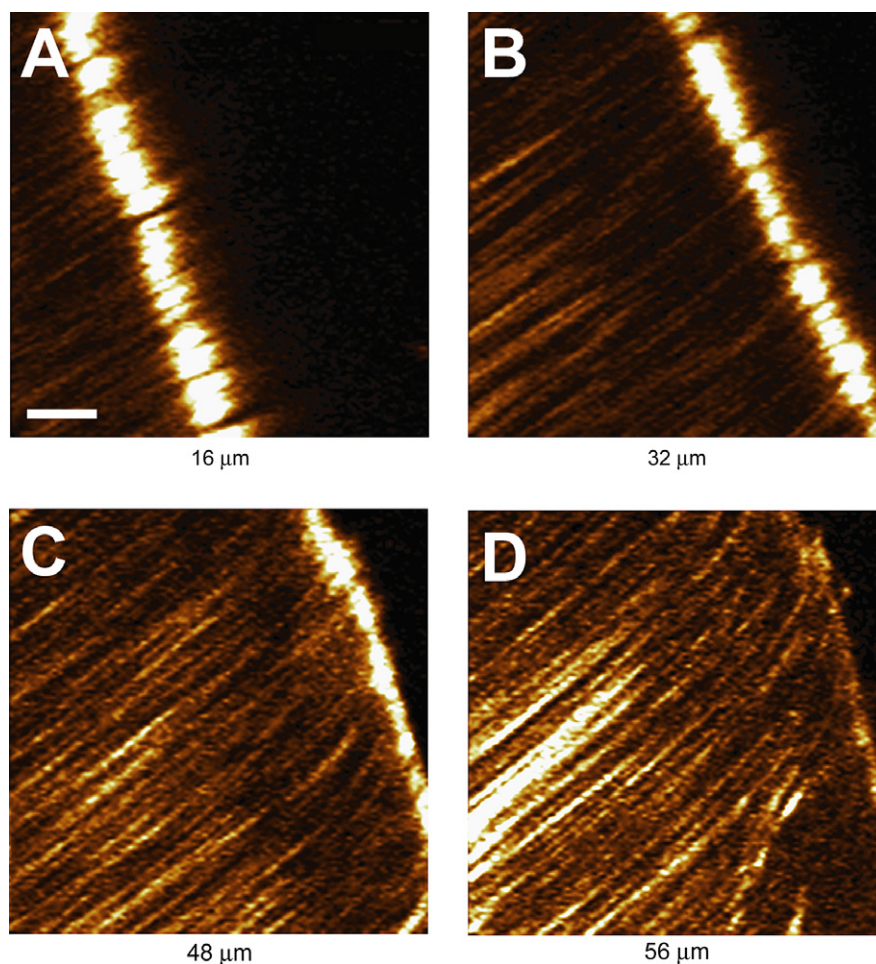


Fig. 3. Second-harmonic microscopy images of the TM's basal HC zone. The Z positions of the optical sections are relative to the stereocilium-imprinted surface, which is referenced as 0 μm . Collagen fibers are arranged in parallel orientation to each other and to the TM surface over the entire thickness of the basal HC zone. Note the intensified band at the edge of the TM sample. This band exists in all sections (A–C) and disappears towards the covering net surface of the TM (D). Scan area is $30 \times 30 \mu\text{m}$, 140×140 pixels. Scale bar, 5 μm . The thickness of the basal HC zone in all tested samples varied between 48 and 56 μm .

We next analyzed the arrangement of the MB collagen fibers at the basal region of the TM (Fig. 5). As in the apical region, the basal collagen fibers are thicker in the MB zone than in the HC zone. In contrast to the apical region, however, we find that the MB zone fibers at the basal region are arranged in parallel orientation with respect to the TM surface. This orientation is preserved throughout the interior of the TM.

Finally, analysis of the collagen fiber arrangements in the limbal zone shows no significant changes relative to the longitudinal zone (apical or basal). The collagen fibers in the limbal zone are arranged in a packed manner. Fig. 6 shows this packed arrangement in the limbal zone at the basal region of the TM. The fibers are parallel to the plane of the TM surface, but appear to be loosely aligned with respect to each other.

Our group, using nano- and microindentation techniques, recently characterized the mechanical properties of the TM along its radial and longitudinal directions (Gueta et al., 2006). In that study, changes in the mechan-

ical properties were supported by SEM analysis of the TM's structure. There were two major shortcomings in the correlation between SEM and mechanical analyses. Whereas the mechanical analysis of the TM was done under physiological conditions and was therefore probably representative of the mechanical properties of the TM's bulk material, the SEM analysis was done on fixed samples, thus yielding structural information only for the TM's surface. In contrast, the SHIM analysis of the TM described in this report provides an insight into the structure of both the surface and the interior of the TM in a physiological environment. It might therefore offer a more realistic correlation between the structure of the TM and its mechanical properties.

In the previous study by our group (Gueta et al., 2006), the most dramatic differences in mechanical properties were found along the entire length of the TM in the HC zone. The stiffness of the TM at the basal region was increased by one order of magnitude relative to the apical region. In line with those findings, we observed here that

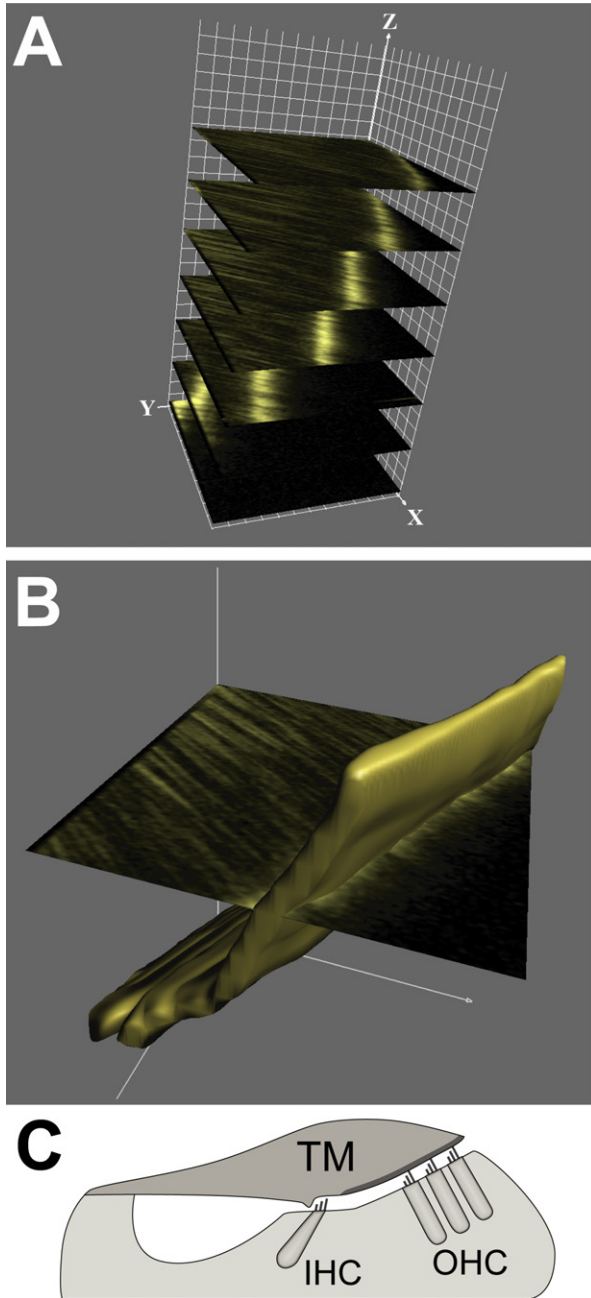


Fig. 4. Z-stack second-harmonic images of the HC zone at the basal region of the TM. (A) Representative sections are presented in 3D, showing the progress of the intensified band along the edge of the TM. (B) A surface-rendered model of the shell-like structure made up of the intensified band. A typical section is shown to demonstrate the position of the parallel collagen fibers with respect to the shell. Note that the bowled shape of the TM is preserved even though the sample is attached to the glass slide at the narrow side (the lower part in the picture). (C) Schematic representation of the organ of Corti, showing the location of the basal OHC shell-like structure (shown as a thick dark line) relative to the outer hair cells in the cochlea.

the HC zone is the region where changes in the arrangements of collagen fibers are the most dramatic. At the TM's apical region the fibers are tilted at an angle with respect to the normal plane of the TM, while at the basal region they are parallel. The mechanical properties of the

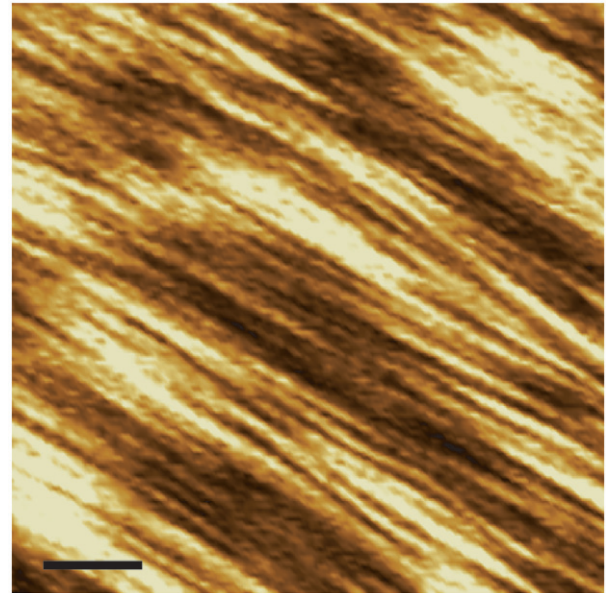


Fig. 5. A typical second-harmonic image of the MB zone at the basal region. The image was acquired at a distance of $32\ \mu\text{m}$ above the stereocilium-imprinted surface of the TM. Identical images are obtained throughout the entire thickness of the sample. Scan area is $30 \times 30\ \mu\text{m}$, 140×140 pixels. Scale bar, $5\ \mu\text{m}$.

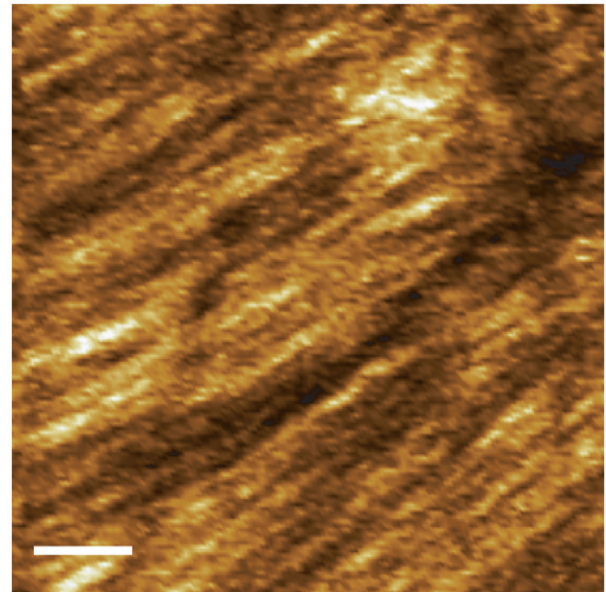


Fig. 6. A representative second-harmonic image of the basal limbal zone. Arrangements of the collagen fibers were similar, not only along the longitudinal direction (basal vs. apical), but also throughout the thickness of the TM. The image was acquired at a distance of $8\ \mu\text{m}$ above the stereocilium-imprinted surface of the TM. Scan area is $30 \times 30\ \mu\text{m}$, 140×140 pixels. Scale bar, $5\ \mu\text{m}$.

TM were measured in that earlier study by application of forces perpendicular to its normal plane. The different orientations of collagen fibers at the basal and apical regions (shown schematically in Fig. 7) are likely to contribute to the observed changes in TM stiffness. Indentation of colla-

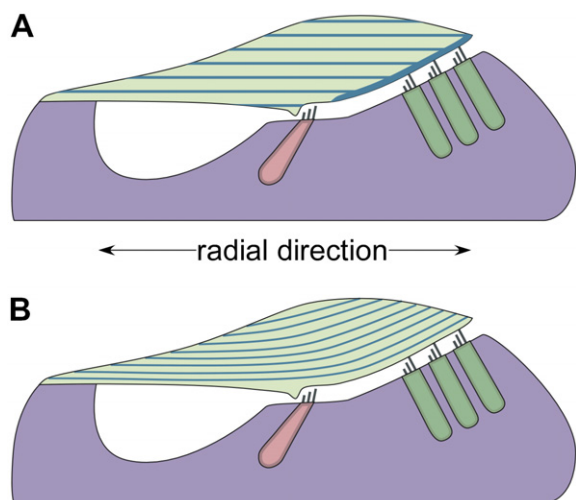


Fig. 7. Schematic representation of the organ of Corti showing arrangements of the collagen fibers inside the TM, based on the results of SHIM analysis. (A) At the basal region of the cochlea the fibers are arranged in parallel orientation and form a shell-like structure at the surface of the TM above the OHCs. (B) In contrast, at the apical region of the cochlea the fibers are arranged in a tilted orientation.

gen fibers that are perpendicular to the direction of the applied force (i.e., at the basal region) requires greater force than that required to indent these fibers when they are partially oriented in the same direction as the applied force (i.e., at the apical region). Moreover, at the edge of the basal HC zone we observe an intensified signal, which corresponds to the merging of several fibers into thick fibers. These tightly packed thick fibers create a shell-like structure, which engulfs the surface of the TM on the side that faces the OHCs (Fig. 4). The shell contributes to the mechanical strength of this zone, as indicated by the fact that the convex structure at the edge is preserved regardless of the orientation of the TM relative to the glass slide. This structure most probably increases the stiffness of the HC zone in the basal region relative to the apical region.

Throughout the longitudinal and radial directions of the TM its biochemical composition is similar (Hasko and Richardson, 1988). Nonetheless, our earlier analysis of the TM's mechanical properties (Gueta et al., 2006) provides supporting evidence for the existence of mechanical coupling between the TM and the stereocilium bundles. In the present work, we demonstrate differences in the suprastructure of TM collagen fibers along the longitudinal and the radial direction. These structural differences are likely to affect those mechanical properties of the TM that are needed in order to promote such a mechanical coupling.

Acknowledgments

We thank Yehudit Hermesh for technical assistance in the surgical procedures performed on the animals. This work was supported in part by the Israel Science Founda-

tion, a grant from the Jean-Jacques Brunshwig Fund for the Molecular Genetics of Cancer, and the Kimmelman Center for Macromolecular Assemblies. I.R. is the incumbent of the Robert Edwards and Roselyn Rich Manson Career Development Chair.

References

- Abnet, C.C., Freeman, D.M., 2000. Deformations of the isolated mouse tectorial membrane produced by oscillatory forces. *Hear. Res.* 144, 29–46.
- Arima, T., Lim, D.J., Kawaguchi, H., Shibata, Y., Uemura, T., 1990. An ultrastructural study of the guinea pig tectorial membrane 'type A' protofibril. *Hear. Res.* 46, 289–292.
- Campagnola, P.J., Loew, L.M., 2003. Second-harmonic imaging microscopy for visualizing biomolecular arrays in cells, tissues and organisms. *Nat. Biotechnol.* 21, 1356–1360.
- Cox, G., Kable, E., Jones, A., Fraser, I., Manconi, F., Gorrell, M.D., 2003. 3-Dimensional imaging of collagen using second harmonic generation. *J. Struct. Biol.* 141, 53–62.
- Freund, I., Deutsch, M., Sprecher, A., 1986. Connective tissue polarity. Optical second-harmonic microscopy, crossed-beam summation, and small-angle scattering in rat-tail tendon. *Biophys. J.* 50, 693–712.
- Glueckert, R., Pfaller, K., Kinnefors, A., Schrott-Fischer, A., Rask-Andersen, H., 2005. High resolution scanning electron microscopy of the human organ of Corti. A study using freshly fixed surgical specimens. *Hear. Res.* 199, 40–56.
- Gueta, R., Barlam, D., Shneck, R.Z., Rouso, I., 2006. Measurement of the mechanical properties of isolated tectorial membrane using atomic force microscopy. *Proc. Natl. Acad. Sci. USA* 103, 14790–14795.
- Hasko, J.A., Richardson, G.P., 1988. The ultrastructural organization and properties of the mouse tectorial membrane matrix. *Hear. Res.* 35, 21–38.
- Jacobson, J., Jacobson, C., Gibson, W., 1990. Hearing loss in Stickler's syndrome: a family case study. *J. Am. Acad. Audiol.* 1, 37–40.
- Legan, P.K., Rau, A., Keen, J.N., Richardson, G.P., 1997. The mouse tectorins. Modular matrix proteins of the inner ear homologous to components of the sperm-egg adhesion system. *J. Biol. Chem.* 272, 8791–8801.
- Legan, P.K., Lukashkina, V.A., Goodyear, R.J., Lukashkin, A.N., Verhoeven, K., Van Camp, G., Russell, I.J., Richardson, G.P., 2005. A deafness mutation isolates a second role for the tectorial membrane in hearing. *Nat. Neurosci.* 8, 1035–1042.
- McGuirt, W.T., Prasad, S.D., Griffith, A.J., Kunst, H.P., Green, G.E., Shpargel, K.B., Runge, C., Huybrechts, C., Mueller, R.F., Lynch, E., King, M.C., Brunner, H.G., Cremers, C.W., Takanosu, M., Li, S.W., Arita, M., Mayne, R., Prockop, D.J., Van Camp, G., Smith, R.J., 1999. Mutations in COL11A2 cause non-syndromic hearing loss (DFNA13). *Nat. Genet.* 23, 413–419.
- Millard, A.C., Campagnola, P.J., Mohler, W., Lewis, A., Loew, L.M., 2003. Second harmonic imaging microscopy. *Methods Enzymol.* 361, 47–69.
- Mohler, W., Millard, A.C., Campagnola, P.J., 2003. Second harmonic generation imaging of endogenous structural proteins. *Methods* 29, 97–109.
- Pfister, M., Thiele, H., Van Camp, G., Fransen, E., Apaydin, F., Aydin, O., Leistschneider, P., Devoto, M., Zenner, H.P., Blin, N., Nurnberg, P., Ozkarakas, H., Kupka, S., 2004. A genotype-phenotype correlation with gender-effect for hearing impairment caused by TECTA mutations. *Cell Physiol. Biochem.* 14, 369–376.
- Slepecky, N.B., Savage, J.E., Cefaratti, L.K., Yoo, T.J., 1992. Electron-microscopic localization of type II, IX, and V collagen in the organ of Corti of the gerbil. *Cell Tissue Res.* 267, 413–418.
- Thalmann, I., Machiki, K., Calabro, A., Hascall, V.C., Thalmann, R., 1993. Uronic acid-containing glycosaminoglycans and

- keratan sulfate are present in the tectorial membrane of the inner ear: functional implications. *Arch. Biochem. Biophys.* 307, 391–396.
- Thalmann, I., Thallinger, G., Crouch, E.C., Comegys, T.H., Barrett, N., Thalmann, R., 1987. Composition and supramolecular organization of the tectorial membrane. *Laryngoscope* 97, 357–367.
- Tsuprun, V., Santi, P., 1997. Ultrastructural organization of proteoglycans and fibrillar matrix of the tectorial membrane. *Hear. Res.* 110, 107–118.
- Ulfendahl, M., Flock, A., Scarfone, E., 2001. Structural relationships of the unfixed tectorial membrane. *Hear. Res.* 151, 41–47.
- Weaver, S.P., Schweitzer, L., 1994. A radial gradient of fibril density in the gerbil tectorial membrane. *Hear. Res.* 76, 1–6.
- Williams, R.M., Zipfel, W.R., Webb, W.W., 2005. Interpreting second-harmonic generation images of collagen I fibrils. *Biophys. J.* 88, 1377–1386.
- Yasui, T., Tohno, Y., Araki, T., 2004. Determination of collagen fiber orientation in human tissue by use of polarization measurement of molecular second-harmonic-generation light. *Appl. Opt.* 43, 2861–2867.
- Yeh, A.T., Hammer-Wilson, M.J., Van Sickle, D.C., Benton, H.P., Zoumi, A., Tromberg, B.J., Peavy, G.M., 2005. Nonlinear optical microscopy of articular cartilage. *Osteoarthritis Cartilage* 13, 345–352.
- Zipfel, W.R., Williams, R.M., Christie, R., Nikitin, A.Y., Hyman, B.T., Webb, W.W., 2003. Live tissue intrinsic emission microscopy using multiphoton-excited native fluorescence and second harmonic generation. *Proc. Natl. Acad. Sci. USA* 100, 7075–7080.